Analyst

ROYAL SOCIETY OF CHEMISTRY

PAPER

View Article Online
View Journal | View Issue

Check for updates

Cite this: *Analyst*, 2021, **146**, 5271

Single-digit *Salmonella* detection with the naked eye using bio-barcode immunoassay coupled with recombinase polymerase amplification and a CRISPR-Cas12a system†

Qiqi Cai,[a] Rui Wang,[b] Zhaohui Qiao *[a] and Wenge Yang[a]

The ability to visually detect low numbers of *Salmonella* in food samples is highly valuable but remains a challenge. Here we present a novel platform for ultrasensitive and visual detection of *Salmonella* Typhimurium by integrating the bio-barcode immunoassay (BCA), recombinase polymerase amplification (RPA), and CRISPR-Cas12a cleavage in a single reaction system (termed as BCA–RPA–Cas12a). In the system, the target bacteria were separated by immunomagnetic nanoparticles and labeled with numerous barcode AuNPs, which carry abundant bio-barcode DNA molecules to amplify the signal. Afterwards, the bio-barcode DNA molecules were amplified by RPA and subsequently triggered the cleavage activity of Cas12a to generate the fluorescence signal. Due to this triplex signal amplification, the BCA–RPA–Cas12a system can selectively detect *Salmonella* Typhimurium at the single-digit level with the naked eye under blue light within 60 min. Meanwhile, this novel platform was successfully applied to detect *Salmonella* Typhimurium in spiked milk samples with a similar sensitivity and satisfactory recovery, indicating its potential application in real samples. Furthermore, in virtue of the versatility of the antibody in the stage of BCA, the BCA–RPA–Cas12a system can be extended to further application in other bacteria detection and food safety monitoring.

Received 25th April 2021,
Accepted 20th July 2021

DOI: 10.1039/d1an00717c

rsc.li/analyst

Published on 21 July 2021. Downloaded by Shanghai Normal University on 3/23/2022 7:39:17 AM.

Introduction

Salmonella Typhimurium (*S*. Typhimurium) is the major cause of foodborne diseases and has become a great threat to human health.[1,2] Eating *S*. Typhimurium infected food may lead to vomiting, diarrhea, abdominal pain, and even death.[3,4] In China, approximately 80% of foodborne pathogen outbreaks are caused by *S*. Typhimurium.[5,6] Therefore, it is vital to develop a sensitive and rapid identification method for *S*. Typhimurium to effectively guarantee food safety for both the food industry and individuals.[7] The conventional culture method for the detection of foodborne pathogens is known as the internationally reliable "gold standard" method,[8,9] but it is labor-intensive and time-consuming, which does not meet the demand for rapid detection.[10] Besides, enzyme-linked immunosorbent assay (ELISA) is widely used for bacteria detection due to its good specificity and high throughput but still suffers from insufficient sensitivity (from 10^4 to 10^5 CFU mL^{-1}).[11–15] In comparison, polymerase chain reaction (PCR) is highly sensitive and needs expensive instruments and well-trained technicians, which is not conducive to on-site applications.[16,17] Therefore, an integrated method combining the superiorities of these methods for sensitive, rapid, and simple detection of *S*. Typhimurium is urgently needed.[18]

The bio-barcode immunoassay (BCA) is a promising detection method equipped with PCR-like sensitivity and ELISA-like specificity. In this strategy, a barcode gold nanoparticle (AuNP) probe is coated with a high density of bio-barcode DNA to amplify the signal and antibody to recognize the target, where the bio-barcode DNA is liable to couple with different amplification techniques to achieve a second-round signal amplification and the antibody endows the probe with high specificity and versatility. Recently, many bio-barcode assays have been developed for rapid detection of foodborne pathogens,[19,20] enterotoxins,[21] hormones,[22] and proteins,[23] and achieved a 1000-fold lower detection limit than conventional ELISA.[24] Due to the easy operation and high efficiency, some isothermal nucleic acid amplification techniques, such as exponential amplification reaction[25] and rolling circle amplification (RCA),[26] have been integrated into bio-barcode assays to achieve sensitive detection. However, these techniques always

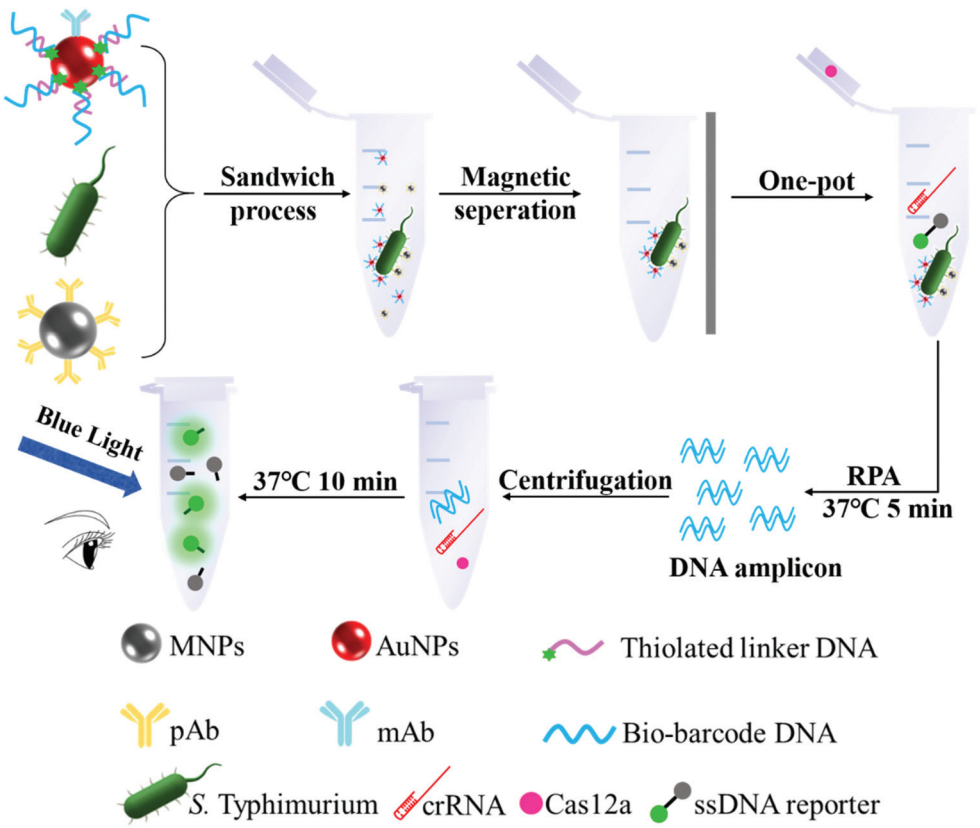
[a]*College of Food and Pharmaceutical Sciences, Ningbo University, Ningbo 315800, China. E-mail: qiaozhaohui@nbu.edu.cn*
[b]*State Key Laboratory of Genetic Engineering, School of Life Sciences, Zhongshan Hospital, Fudan University, Shanghai, 200432, China*
†Electronic supplementary information (ESI) available. See DOI: 10.1039/d1an00717c

Published on 21 July 2021. Downloaded by Shanghai Normal University on 3/23/2022 7:39:17 AM.

need too much amplification time (*e.g.*, 90 min for RCA), an expensive fluorescence spectrophotometer, and a complex step of releasing DNA from the surface of barcode AuNPs.[27–29]

Recently, recombinase polymerase amplification (RPA) has shown promise as a representative isothermal amplification technique with the characteristics of rapid detection, amplification at a relatively low temperature (37–42 °C), high sensitivity, and high accuracy. Thus, RPA has been successfully used in the detection of various pathogenic bacteria and achieved the detection limits of 10–10^2 CFU mL^{-1} within 20 min.[30–34] Although simple and rapid, these methods are still challenged by some issues, such as aerosol contamination and unsatisfactory sensitivity for some "zero-tolerance" pathogens in the field or poor areas. Recently, one-pot assays integrated with CRISPR-Cas12a and nucleic acid isothermal amplification techniques have been demonstrated to be promising approaches to reduce aerosol contamination. Many one-pot detection methods based on RPA coupled CRISPR-Cas12a have been established to detect pathogens in clinical and food samples with high sensitivities.[35–37] Yet, it is still difficult to distinguish the early stage of pathogen contamination in the field or poor areas without expensive instruments and more signal amplification techniques are needed.[38]

Herein, we combine the BCA with RPA and a CRISPR-Cas12a system to achieve a rapid, ultrasensitive, and visual detection of *S*. Typhimurium, where the detection platform is termed as a BCA–RPA–Cas12a system. In this system (Scheme 1), barcode AuNPs were functionalized with a monoclonal antibody and numerous bio-barcode DNA molecules and magnetic nanoparticles (MNPs) were modified with a polyclonal antibody for immunomagnetic separation. Initially, the barcode AuNP and MNP probes were attached on the surface of *S*. Typhimurium to form a "MNP–bacteria–AuNP" sandwich structure. Due to the ingenious design of the barcode AuNPs, the sandwich structure was directly incubated with RPA–Cas12a one-pot reagents to perform signal amplification and visualized readout without the step of releasing bio-barcode DNA. In the whole process, triplex signal amplification has been used to enhance the sensitivity of detection. Firstly, hundreds of AuNPs are coated with a large amount of bio-barcode DNA attached on the surface of bacteria to amplify the signal of bacterial cells into that of numerous bio-barcode DNA molecules.[39] Secondly, the bio-barcode DNA can be directly exponentially amplified *via* RPA within several minutes to accomplish the second round of signal amplification. Finally, the amplicon of RPA was recognized by crRNA and successively activated the high-efficiency Cas12a-catalyzed cleavage of a dual-labeled single strand (ssDNA) reporter. Therefore, after three rounds of signal amplification, the fluorescence of the detection system remarkably increased in the presence of the target bacteria and can be easily visualized by the naked eye. In contrast, if *S*. Typhimurium is absent, no AuNP probes will



Scheme 1 Scheme of the BCA–RPA–Cas12a system for single-digit cell detection with the naked eye.

This journal is © The Royal Society of Chemistry 2021

Published on 21 July 2021. Downloaded by Shanghai Normal University on 3/23/2022 7:39:17 AM.

be separated along with magnetic nanoparticles and no fluorescence enhancement will be triggered at all.

Experimental

Materials and apparatus

Streptavidin magnetic nanoparticles (SA-MNPs) were purchased from Ocean NanoTech (San Diego, CA, USA). Phosphate buffered saline (PBS), bovine serum albumin (BSA), and RNase-free ddH_2O were purchased from Sangon Biotech (Shanghai, China). Gold chloride trihydrate ($HAuCl_4 \cdot 3H_2O$), trisodium citrate dihydrate, sodium carbonate (Na_2CO_3), dithiothreitol (DTT), and D-biotin were purchased from Solarbio (Beijing, China). The TwistAmp Basic Kit used for the RPA reaction was purchased from TwistDx (England). EnGenLba Cas12a and NEBuffer 2.1 were purchased from New England Biolabs (Ipswich, MA, UK). All oligonucleotide sequences (Table S1†) were designed according to the a previous work[40] and synthesized by Sangon Biotech (Shanghai, China). Electrophoresis images were captured and analyzed using a Bio-Rad Gel Doc XR+ system (Bio-Rad, Richmond, CA, USA). The fluorescence was observed under a simple blue light LED (460–485 nm) The instrument used for UV-vis and fluorescence spectroscopy experiments was a SpectraMax i3 Multi-Mode Microplate Reader (Molecular Devices, USA). All other buffers were prepared using ultrapure water (>18.25 MΩ cm) from a Milli-Q® water purification system (Millipore, Billerica, MA, USA).

Preparation of AuNPs

AuNPs were synthesized using the citrate-reduction method. Briefly, 100 mL of 1 mM $HAuCl_4$ aqueous solution in an Erlenmeyer flask was heated to boiling under stirring conditions. Next, 10 mL of 38.8 mM trisodium citrate aqueous solution was added into the Erlenmeyer flask. When the mixed solution color turned from faint yellow to deep red, the heating button was turned off and the solution was stirred for a further 15 min. After being naturally cooled, the resultant AuNP colloids were stored at 4 °C.

Preparation of barcode AuNPs

The monoclonal antibody (mAb) and thiolated oligonucleotides were conjugated onto AuNPs using a freezing-based labeling method on the basis of literature procedures.[41] Firstly, the pH of 1 mL of AuNP solution was adjusted to 7.4 with 25 mM Na_2CO_3. Then, 100 μL of 1 mg mL^{-1} mAb against *S.* Typhimurium and 3 μM thiolated linker DNA were added to the AuNP solution and frozen for 15 min at −80 °C. Afterwards, the mixture was thawed and the supernatant was discarded after centrifugation (9000 rpm, 15 min), and then the particles were resuspended in 1 mL of PBS (0.01 M, pH 7.4). Next, 3 μM bio-barcode DNA was added and hybridized with the linker DNA for a further 15 min at −80 °C. Subsequently, the mixture was added into the BSA (1%) solution and incubated for 60 min. After centrifugation, the supernatant was discarded and the barcode AuNPs were resuspended in 1 mL of PBS.

Preparation of MNP probes

Two hundred microliter of 0.5 mg mL^{-1} biotinylated polyclonal antibody (pAb) against *S.* Typhimurium was added to 200 μL of SA-MNPs (1 mg mL^{-1}) to form complexes under shaking at room temperature. After incubating for 30 min, 40 μL of D-biotin (10 μM) was added to block the unbound sites of SA-MNPs. After incubation for 30 min, the mixture was washed three times with PBST (0.01 M PBS, containing 0.01% Tween-20) and suspended in 200 μL of PBS to form MNP probes, which were stored at 4 °C.

Dot enzyme-linked immunosorbent assay (Dot-ELISA) procedure

Dot-ELISA was performed as follows: notably, the barcode AuNPs used in this section were modified with biotinylated bio-barcode DNA for signal output. Briefly, approximately 5.0 μL of BSA (2%) and 10^3 CFU mL^{-1} *S.* Typhimurium were spotted onto a nitrocellulose membrane marked as dot A (2% BSA), dot B (10^3 CFU mL^{-1} *S.* Typhimurium), and dot C (10^3 CFU mL^{-1} *S.* Typhimurium), respectively. After being air-dried at room temperature (RT), the membrane was soaked for 30 min in blocking buffer (5% skimmed milk). Next, dots A and C were incubated in barcode AuNP solution for 45 min, while dot B was incubated in bare AuNP solution. After three times washing with PBST, the appearance of three dots was observed. Subsequently, the membrane was incubated for another 25 min in 0.01 mg mL^{-1} streptavidin–horseradish peroxidase (SA-HRP) solution. After three times washing with PBST, the membrane was immersed in a 4-chloro-1-naphthol (4C1N) substrate for color development.

Preparation of a MNP–bacteria–AuNP sandwich structure

First, 3 μL of MNP probes were added to sterile centrifuge tubes. Then 200 μL of the *S.* Typhimurium sample with concentrations ranging from 10^0 to 10^6 CFU mL^{-1} diluted in PBS and 20 μL of barcode AuNPs were sequentially added to the tubes and incubated for 45 min at RT under gentle shaking. After the reaction, the mixture was washed three times with PBST using a magnet. After the final wash, the formed MNP–bacteria–AuNP sandwich structure containing the bio-barcode DNA strands was resuspended in 3 μL of RNase-free ddH_2O.

One-pot detection

One-pot detection combined RPA preamplification with CRISPR-Cas12a cleavage detection in the one-pot system. Briefly, the 25 μL one-pot detection system contained 14.75 μL of rehydration buffer, one-sixth of a lyophilized enzyme pellet, 0.5 μL of 10 μM forward primer, 0.5 μL of 10 μM reverse primer, 1.25 μL of 10 μM crRNA, 0.5 μL of 10 μM quenched fluorescent ssDNA reporter, 10 U of RNase inhibitor, 2 μL of NEBuffer 2.1, 0.53 μL of 280 mM magnesium acetate (MgOAc), 3 μL of sandwich structure, 1.25 μL of 5 μM Cas12a, and RNase-free ddH_2O up to 25 μL. Cas12a was initially added on

Published on 21 July 2021. Downloaded by Shanghai Normal University on 3/23/2022 7:39:17 AM.

the tube lid. After the RPA reaction for 5 min, Cas12a was mixed with the amplicons by centrifugation and incubated for 10 min at 37 °C. Afterwards, a bright green fluorescence signal could be observed by the naked eye under blue light LED irradiation.

Milk sample preparation

Milk samples were purchased from a local market in Ningbo. *S.* Typhimurium was added to the milk samples to achieve different concentrations from 10^6 to 10^0 CFU mL^{-1} using 10-fold serial dilutions. Then, the milk samples were detected using the proposed method. Besides, the traditional plate-counting method for assaying the bacteria in the samples served as the standard method.

Results and discussion

BCA–RPA–Cas12a system

Barcode AuNPs were synthesized and then characterized by UV-vis spectroscopy and transmission electron microscopy. As shown in Fig. 1A, the maximum absorbance of the bare AuNPs was 518 nm. After the attachment of the antibody, thiolated linker DNA strands, and bio-barcode DNA strands to the AuNPs, the maximum absorbance of the AuNPs was red-shifted from 518 to 524 nm. Afterwards, the formation of barcode AuNPs was further evaluated by Dot-ELISA. As shown in the left side of Fig. 1B, dot C (*S.* Typhimurium + barcode AuNPs) appeared red after incubation with barcode AuNPs while the control dots, which were dot A (BSA + barcode AuNPs) and dot B (*S.* Typhimurium + bare AuNPs), showed no color at all. This result suggested the successful modification of the antibody on the surface of AuNPs. Additionally, these dots were further incubated with SA-HRP to verify the modification of bio-barcode DNA *via* the interaction of biotin and streptavidin. As shown in the right side of Fig. 1B, dot C became purple-gray while there was still no color in dots A and B. This indicated that the AuNPs were modified with biotinylated bio-barcode DNA. Therefore, the barcode AuNPs modified with the antibody and bio-barcode DNA can be successfully prepared by the proposed method.

Then, we verified that the bio-barcode DNA on barcode AuNPs can be amplified by RPA *via* agarose electrophoresis. As shown in Fig. 1C, the products of barcode AuNPs showed a single band clearly (lane 1, 89 bp), while the product of linker AuNPs (lane 2) hardly showed any band, indicating that the bio-barcode DNA on barcode AuNPs can be efficiently amplified by RPA. Furthermore, the cleavage activity of Cas12a triggered by the RPA products of barcode AuNPs was evaluated. As shown in Fig. 1D, the fluorescence intensity of the barcode AuNP–RPA–Cas12a sample was extremely high and can be easily observed by the naked eye, while the linker AuNP–RPA–Cas12a sample showed low fluorescence intensity and can be hardly observed by the naked eye. Therefore, the bio-barcode DNA can be successfully amplified by the RPA reaction and triggered the cleavage activity of Cas12a.

After the fabrication of barcode AuNPs, the MNP–bacteria–AuNP sandwich structure was formed and further character-

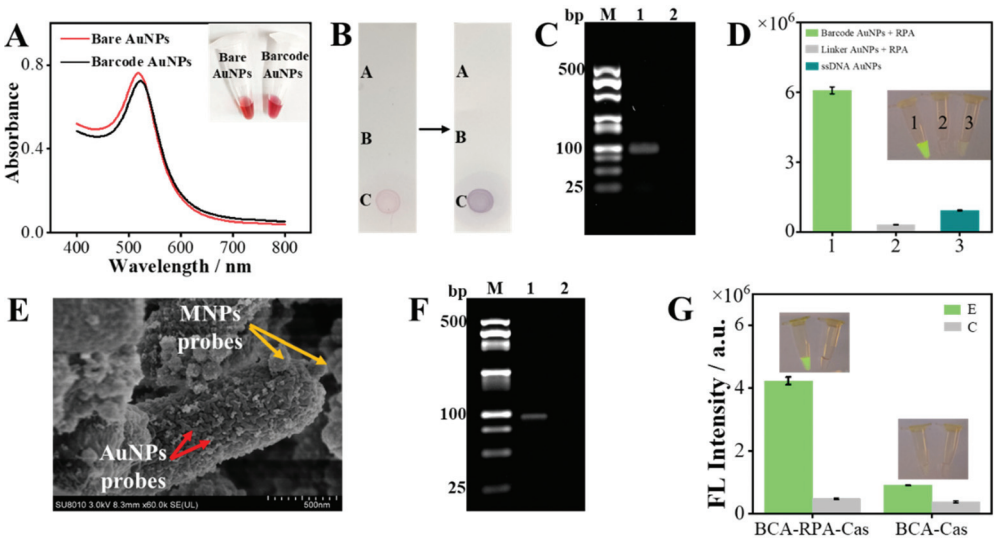


Fig. 1 Characterization of the BCA–RPA–Cas12a system. (A) UV-vis spectra of bare AuNPs (red line) and barcode AuNPs (black line). (B) Image of Dot-ELISA. Left: dot A: BSA + barcode AuNPs; dot B: *S.* Typhimurium + bare AuNPs; and dot C: *S.* Typhimurium + barcode AuNPs; right: dots A, B, and C were incubated with SA-HRP and 4-CN. (C) Agarose gel electrophoresis image of RPA products of different samples. Lane M: marker; lane 1: barcode AuNPs + RPA; and lane 2: linker AuNPs + RPA. (D) Fluorescence intensities of barcode AuNPs + RPA (1), linker AuNPs + RPA (2), and ssDNA (3) triggered Cas12a system. (E) SEM image of the MNP–bacteria–AuNP sandwich structure. (F) Agarose gel electrophoresis image of RPA products of different samples. Lane M: marker. Lane 1: *S.* Typhimurium positive sample (89 bp). Lane 2: negative control. (G) Detection of *S.* Typhimurium based on the BCA–RPA–Cas12a and BCA–Cas12a systems and visual detection under blue light irradiation. The concentration of *S.* Typhimurium was 10^3 CFU mL^{-1}.

 This journal is © The Royal Society of Chemistry 2021

Published on 21 July 2021. Downloaded by Shanghai Normal University on 3/23/2022 7:39:17 AM.

ized by scanning electron microscopy (SEM). As shown in Fig. 1E, the rod-shaped *S.* Typhimurium was covered with numerous barcode AuNP probes and spherical MNPs through the specific binding of antibodies and antigens. In addition, the size of MNP probes was 150 nm according to the description and that of barcode AuNP probes was about 12.5 nm, which was consistent with the result analyzed by transmission electron microscopy (Fig. S1†).

Subsequently, the RPA amplification performance of bio-barcode DNA on the sandwich structure was investigated by the analysis of *S.* Typhimurium with a concentration of 10^3 CFU mL^{-1}. As shown in the result of electrophoresis (Fig. 1F), the positive sample showed a single band clearly (lane 1, 89 bp), while the negative control (PBS) hardly showed any band (lane 2), indicating that the bio-barcode DNA of the sandwich structure was amplified by the RPA reaction successfully. Finally, the whole principle of the proposed method was evaluated by the detection of *S.* Typhimurium (10^3 CFU mL^{-1}). In the whole process, the RPA and Cas12a cleavage were integrated into a one-pot reaction to simplify the operation and save time according to a previous report.[35] As shown in Fig. 1G, in the BCA–RPA–Cas12a system, the fluorescence intensity of the negative control was extremely low and can hardly be observed by the naked eye, while in the presence of *S.* Typhimurium, the fluorescence intensity significant increased (8.8-fold of the negative control) and can be easily observed by the naked eye, demonstrating that the fluorescent probes were cut efficiently by RPA amplicon activated Cas12a. These results strongly confirmed the feasibility of the bio-barcode immunoassay coupled with RPA and CRISPR-Cas12a for the fluorescence detection of *S.* Typhimurium with the naked eye.

According to a previous work, ssDNA can also trigger the cleavage activity of Cas12a, even though the reaction rate of the ssDNA activator is much slower than that of dsDNA.[42] To verify the performance of the ssDNA activator, ssDNA modified AuNPs were synthesized and directly triggered the cleavage activity of Cas12a. As we can see from Fig. 1D, the ssDNA directly triggered sample (3) without the RPA reaction showed faint fluorescence in the image, indicating that the ssDNA on the surface of AuNPs can also activate the cleavage. However, the intensity was only 15% of barcode AuNPs with RPA. When it is used for the detection of bacteria (BCA–Cas12a system), the intensity of the positive sample was rather low and only 21% of the intensity of the BCA–RPA–Cas12a system (Fig. 1G). Therefore, the RPA reaction is necessary for the visual detection of ultralow numbers of bacteria.

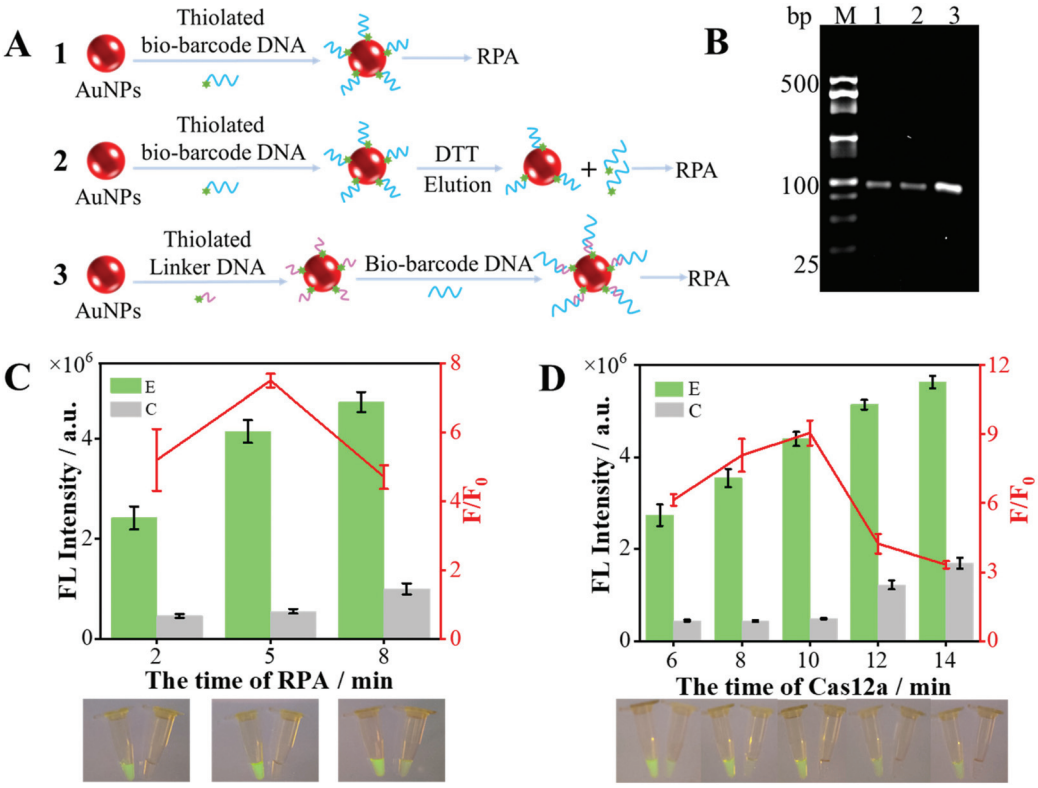


Fig. 2 (A) Principle of three methods for preparing the barcode AuNPs and their RPA amplification efficiency (B). 1: Direct method; 2: elution method; and 3: indirect method. Optimization of the time of the RPA reaction (C) and CRISPR-Cas12a system (D). The concentration of *S.* Typhimurium was 10^3 CFU mL^{-1}. Bar graph: fluorescence intensity of the positive sample (green) and the negative control (gray). Red curve: F/F_0 (the fluorescence intensity of positive sample *vs.* negative control). Bottom row: visual detection under blue light irradiation, photographed using a smartphone.

Published on 21 July 2021. Downloaded by Shanghai Normal University on 3/23/2022 7:39:17 AM.

Optimization of detection conditions

There are three methods for preparing barcode AuNPs including the direct method, elution method, and indirect method (Fig. 2A). In detail, the direct method means that the bio-barcode DNA was modified on AuNPs *via* the Au–S bond and was directly amplified by RPA. The elution method means that the bio-barcode DNA was released from the surface of AuNPs by DTT and then amplified by RPA. Finally, the indirect method means that the bio-barcode DNA was modified on AuNPs with the help of a thiolated linker DNA and was directly amplified by RPA without elution. The amplification efficiency of RPA for barcode AuNPs prepared by different methods was investigated. As shown in Fig. 2B, lanes 1, 2, and 3 show the electrophoresis images of RPA products for the direct method, elution method, and indirect method, respectively. The electrophoresis images of lanes 1 and 2 were much weaker than that of lane 3, indicating that the RPA efficiency of the indirect method is the highest. We suspect that the fixation of one end of the bio-barcode DNA on the surface of AuNPs has an adverse effect on the process of RPA in the direct method. In terms of the elution method, we suspect that the low elution efficiency of thiolated bio-barcode DNA on the surface of AuNPs may lead to poor amplification efficiency after excluding the influence of the additional reagent (DTT) in the RPA process (Fig. S3†). Therefore, we adopted the indirect method to prepare the barcode AuNPs, where the bio-barcode DNA attached on the surface of AuNPs with the help of a thiolated linker DNA and can be easily released in the process of RPA by the elongation of the complementary sequence of bio-barcode DNA.

In the process of RPA, the reaction time directly affects the amplification efficiency. In the proposed method, the low amplification efficiency would lead to poor sensitivity and the ultrahigh efficiency would produce a high background. Therefore, the reaction time for RPA ranging from 2 min to 8 min was carefully optimized. As shown in Fig. 2C, the fluorescence intensity of the positive sample and the negative control increased along with the increase of the reaction time and the background signal became obvious at a time of 8 min. Thus, 5 min was used as the optimal RPA reaction time in the subsequent experiments. Furthermore, the reaction time of Cas12a-mediated cleavage activity was optimized with test values of 6, 8, 10, 12, and 14 min. As shown in Fig. 2D, the reaction time of 10 min yielded an obvious distinction between the positive sample and the negative control. Thus, a reaction time of Cas12a-mediated cleavage activity of 10 min was chosen for further experiments.

Sensitivity of the assay

For the evaluation of the sensitivity of the BCA–RPA–Cas12a system for *S.* Typhimurium detection, a series of gradient dilution concentrations of *S.* Typhimurium from 10^0 to 10^6 CFU mL^{-1} were prepared. Meanwhile, no-*S.* Typhimurium was used as the negative control. As shown in Fig. 3A, the fluorescence intensity increased gradually when the concentration of the target bacteria increased from 10^0 to 10^6 CFU mL^{-1}, and

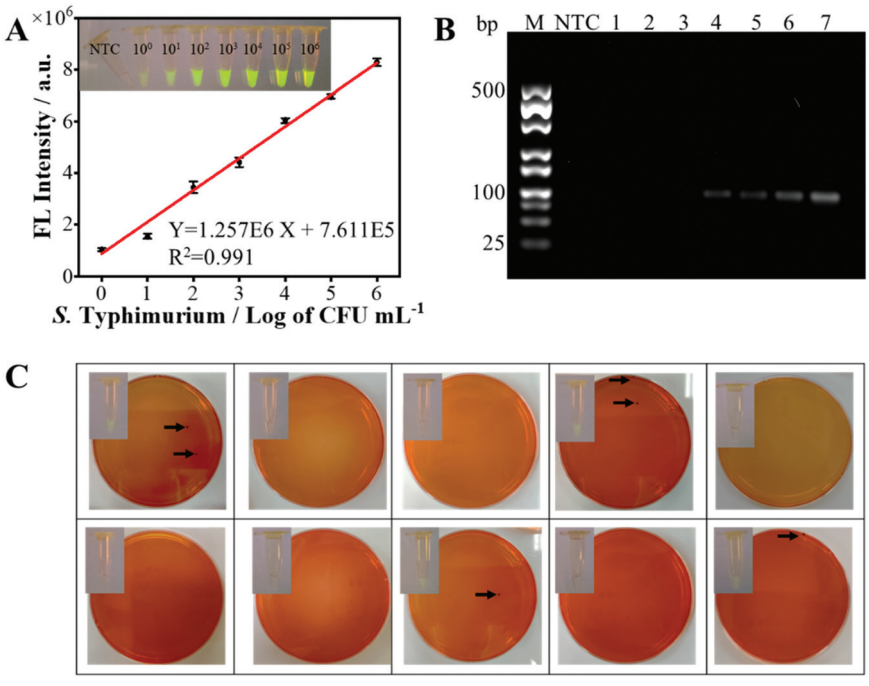


Fig. 3 Sensitivity of *S.* Typhimurium detection using the BCA–RPA–Cas12a system. (A) Linear relationship between the fluorescence intensity and the logarithm of *S.* Typhimurium concentrations (10^0–10^6 CFU mL^{-1}). (B) Agarose gel electrophoresis image of RPA products with different concentrations of *S.* Typhimurium. Lane M: molecular weight marker. Lanes 1–7 show 10^0–10^6 CFU mL^{-1} *S.* Typhimurium, respectively. NTC, negative control. (C) BCA–RPA–Cas12a detection of *S.* Typhimurium at single-digit numbers, which was confirmed with cell plating.

 This journal is © The Royal Society of Chemistry 2021

Published on 21 July 2021. Downloaded by Shanghai Normal University on 3/23/2022 7:39:17 AM.

the corresponding regression equation is $Y = 1.257 \times 10^{-6} X + 7.611 \times 10^{-5}$ ($R^2 = 0.991$), where X is the concentration of bacteria in log CFU mL^{-1} and Y is the value of the fluorescence intensity. The LOD of the detection system with the naked eye was 1 CFU mL^{-1}, which is much lower than that of electrophoresis (10^3 CFU mL^{-1}, Fig. 3B). To further verify the sensitivity, samples with ultralow concentrations of the target bacteria were detected using the proposed method. The whole volume of 2 mL bacteria solution with a concentration of 3 ± 1 bacteria per mL is used for BCA–RPA–Cas12a detection. The solution was divided into 10 tubes of 200 μL and detected by the proposed method. After BCA–RPA–Cas12a detection, the bacteria sandwich structures were magnetically separated and used for plate counting. As shown in Fig. 3C, there were only four tubes that showed naked-eye observed fluorescence, with each tube containing one to two bacteria counted by cell plate culture. This result indicated that the BCA–RPA–Cas12a system can detect single-digit bacteria with the naked eye in the all-or-none response mode.

Specificity of the assay

In real-world samples, it is found that *S.* Typhimurium is usually mixed with many other bacterial species; thus it is important to specifically distinguish *S.* Typhimurium from other bacteria. To evaluate the specificity of the proposed method, the responses toward some non-target bacteria, such as *E. coli* (a typical Gram-negative bacteria) and *L. monocytogenes* (a typical Gram-positive bacteria), at a higher concentration (10^3 CFU mL^{-1}) were investigated. As shown in Fig. 4, there were hardly any fluorescence signal observed in the non-target bacteria and negative control. In contrast, the positive sample and the mixture sample of three bacteria with a ratio of 1 : 1 : 1 showed a strong and similar fluorescence signal, which suggested the good specificity of this proposed method. We speculated that this high specificity mainly comes from the high specificity of the monoclonal antibody on the barcode AuNPs and the sharp specificity of the cleavage reaction of Cas12a.

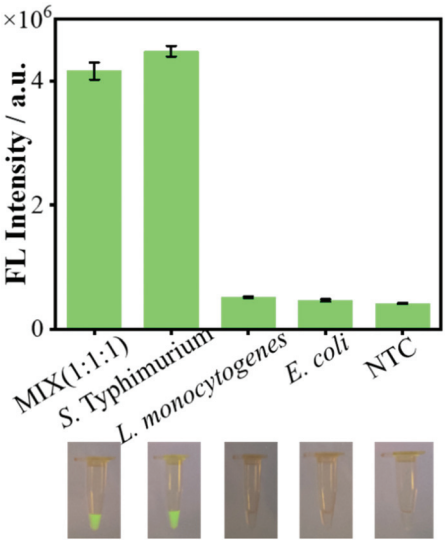


Fig. 4 Specificity of *S.* Typhimurium detection using the BCA–RPA–Cas12a system. Top row: fluorescence intensity of MIX (*S.* Typhimurium : *E. coli* : *L. monocytogenes* = 1 : 1 : 1), 10^3 CFU mL^{-1} *S.* Typhimurium, *E. coli*, *L. monocytogenes*, and negative control. Bottom row: visual detection under blue light irradiation, photographed using a smartphone. NTC, negative control.

Detection of *S.* Typhimurium in real samples

To further evaluate the applicability of the proposed method, *S.* Typhimurium in spiked milk samples was detected and the results are shown in Fig. 5. The fluorescence intensity proportionately increased as the concentration of *S.* Typhimurium increased and the linear regression equation is $Y = 1.101 \times 10^{-6} X + 1.194 \times 10^{-6}$ ($R^2 = 0.988$). As we can see, the LOD of the proposed method is still 1 CFU mL^{-1} in the food matrix, indicating that the complex food samples can hardly affect the performance of the proposed method. This might be caused by the great separation efficiency of MNPs toward *S.* Typhimurium. Thus, the results demonstrated that our method has good stability in milk samples and showed the potential for application in food samples. Subsequently, we further performed recovery experiments at different spiked *S.* Typhimurium concentrations in milk. As shown in Table 1,

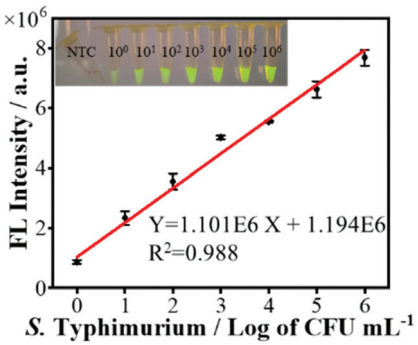


Fig. 5 Application of *S.* Typhimurium detection using the BCA–RPA–Cas12a system. Linear relationship between the fluorescence intensity and the logarithm of *S.* Typhimurium concentrations (10^0–10^6 CFU mL^{-1}) in milk samples. NTC, negative control.

Table 1 The results of recovery experiments for the detection of *S.* Typhimurium in milk samples using the proposed method

Sample	Spiked (CFU mL^{-1})	Fluorescence (a.u.)	Detected (CFU mL^{-1})	Recovery (%)
S_1	1×10^2	3353274	91	91.45%
S_2	1×10^2	3464894	115	115.50%
S_3	5×10^2	4242848	588	117.54%
S_4	5×10^2	4128743	463	92.59%
S_5	1×10^3	4464824	935	93.49%
S_6	1×10^3	4528739	1069	106.86%
S_7	5×10^3	5172843	4110	82.20%
S_8	5×10^3	5329480	5703	114.06%
S_9	1×10^4	5563948	9313	93.13%
S_{10}	1×10^4	5702834	12 451	124.51%

Published on 21 July 2021. Downloaded by Shanghai Normal University on 3/23/2022 7:39:17 AM.

the recovery for different concentrations (1×10^2–1×10^4 CFU mL^{-1}) of *S.* Typhimurium in milk samples ranged from 82.20% to 124.51%, and the average recovery was 103.13%, indicating that the proposed BCA–RPA–Cas12a system is applicable for the detection of *S.* Typhimurium in food samples.

Conclusions

In this study, a novel BCA–RPA–Cas12a system was developed for the simple, rapid, ultrasensitive, and visual detection of *S.* Typhimurium. Due to the synergy of three successive signal amplification steps, the proposed method can detect as low as single-digit *S.* Typhimurium cells with the naked eye within 60 min. In addition, this method achieved good specificity of different pathogenic bacteria due to the high specificity of the monoclonal antibody and showed good performance in practical sample analysis. Compared with previous detection methods (Table S2†), this platform possesses a series of distinctive advantages. First, compared with other BCA methods, the proposed BCA–RPA–Cas12a system skips the bio-barcode DNA releasing step by introducing a linker DNA and RPA, which significantly simplify the process and reduce the loss of bio-barcode DNA. Secondly, superior to the widely studied dual signal amplification strategies based on nucleic acid amplification and collateral cleavage activity of CRISPR-Cas12a, the bio-barcode strategy amplifies a small number of the target cells into numerous bio-barcode DNA molecules by several orders of magnitude. This amplification will be further enlarged in the next two rounds of signal amplification, which enables single-digit cell visualized fluorescence enhancement. Thirdly, compared with other visual counterparts, this proposed method used the RPA–Cas12a system in a one-pot reaction and the fluorescence signal could be detected by the naked eye, which effectively reduces the risk of aerosol contamination. Finally, in virtue of the versatility of the antibody, the application range of CRISPR-Cas12a-based biosensors can be extended from nucleic acid targets to non-DNA targets. Therefore, this method holds great potential for further application in other bacteria detection, food safety monitoring, or clinical diagnostics.

Author contributions

Qiqi Cai: Conceptualization, methodology, validation, formal analysis, investigation, data curation, writing – original draft, and writing – review and editing. Rui Wang: Conceptualization and writing – review and editing. Zhaohui Qiao: Resources, supervision, writing – review and editing, project administration, and funding acquisition. Wenge Yang: Investigation and writing – review and editing.

Conflicts of interest

The authors declare no competing financial interest.

Acknowledgements

This work was supported by the National Natural Science Foundation of China (Grant No. 32001773), the Zhejiang Provincial Natural Science Foundation of China (Grant No. LQ20C200008), the Ningbo Civil Public Welfare Technology Application Research Project (Grant No. 202002N3064), and the Zhejiang Province Public Welfare Technology Application Research Project (LGN20C200013 and LGN19C200010).

Notes and references

1 J. M. Whichard, K. Gay, J. E. Stevenson, K. J. Joyce, K. L. Cooper, M. Omondi, F. Medalla, G. A. Jacoby and T. J. Barrett, *Emerging Infect. Dis.*, 2007, **13**, 1681–1688.
2 M. Furukawa, N. Goji, T. W. Janzen, M. C. Thomas, D. Ogunremi, B. Blais, N. Misawa and K. K. Amoako, *Can. J. Microbiol.*, 2018, **64**, 75–86.
3 A. Haraga, M. B. Ohlson and S. I. Miller, *Nat. Rev. Microbiol.*, 2008, **6**, 53–66.
4 S. E. Majowicz, J. Musto, E. Scallan, F. J. Angulo, M. Kirk, S. J. O'Brien, T. F. Jones, A. Fazil, R. M. Hoekstra and B. Int Collaboration Enteric Dis, *Clin. Infect. Dis.*, 2010, **50**, 882–889.
5 M. Mangal, S. Bansal, S. K. Sharma and R. K. Gupta, *Crit. Rev. Food Sci. Nutr.*, 2016, **56**, 1568–1584.
6 U. Ryan, N. Hijjawi and L. Xiao, *Int. J. Parasitol.*, 2018, **48**, 1–12.
7 P. Preechakasedkit, W. Siangproh, N. Khongchareonporn, N. Ngamrojanavanich and O. Chailapakul, *Biosens. Bioelectron.*, 2018, **102**, 27–32.
8 P. Poltronieri, V. Mezzolla, E. Primiceri and G. Maruccio, *Foods*, 2014, **3**, 511–526.
9 Z. Zhang, J. Zhou and X. Du, *Micromachines*, 2019, **10**, 222.
10 D. J. You, K. J. Geshell and J.-Y. Yoon, *Biosens. Bioelectron.*, 2011, **28**, 399–406.
11 E. Galikowska, D. Kunikowska, E. Tokarska-Pietrzak, H. Dziadziuszko, J. M. Los, P. Golec, G. Wegrzyn and M. Los, *Eur. J. Clin. Microbiol. Infect. Dis.*, 2011, **30**, 1067–1073.
12 C. M. J. Ferguson, N. A. Booth and E. J. Allan, *Lett. Appl. Microbiol.*, 2000, **31**, 390–394.
13 J. Chen and B. Park, *Int. J. Food Microbiol.*, 2018, **267**, 1–8.
14 W. Wu, J. Li, D. Pan, J. Li, S. Song, M. Rong, Z. Li, J. Gao and J. Lu, *ACS Appl. Mater. Interfaces*, 2014, **6**, 16974–16981.
15 Y. Wang and J. K. Salazar, *Compr. Rev. Food Sci. Food Saf.*, 2016, **15**, 183–205.
16 S. Clais, G. Boulet, M. Van Kerckhoven, E. Lanckacker, P. Delputte, L. Maes and P. Cos, *Lett. Appl. Microbiol.*, 2015, **60**, 79–84.
17 R. Y. C. Kong, S. K. Y. Lee, T. W. F. Law, S. H. W. Law and R. S. S. Wu, *Water Res.*, 2002, **36**, 2802–2812.
18 E. Yang, W. Liao, Q. Lin, H. An, D. Li, F. Wei and Y. Duan, *Anal. Chem.*, 2020, **92**, 8090–8096.

 This journal is © The Royal Society of Chemistry 2021

Published on 21 July 2021. Downloaded by Shanghai Normal University on 3/23/2022 7:39:17 AM.

19 X. Li, C. Zhao, Y. Liu, Y. Li, F. Lian, D. Wang, Y. Zhang, J. Wang, X. Song, J. Li, Y. Yang and K. Xu, *Analyst*, 2019, **144**, 2704–2715.
20 K. Cihalova, D. Hegerova, A. M. Jimenez, V. Milosavljevic, J. Kudr, S. Skalickova, D. Hynek, P. Kopel, M. Vaculovicova and V. Adam, *J. Pharm. Biomed. Anal.*, 2017, **134**, 325–333.
21 Y. Xu, B. Huo, C. Li, Y. Peng, S. Tian, L. Fan, J. Bai, B. Ning and Z. Gao, *Food Chem.*, 2019, **283**, 338–344.
22 H. Lee, K. H. Kim and K. H. Lee, *Sens. Actuators, B*, 2019, **282**, 399–407.
23 A. Amini, M. Kamali, B. Amini, A. Najafi, A. Narmani, L. Hasani, J. Rashidiani and H. Kooshki, *Int. J. Biol. Macromol.*, 2019, **124**, 1256–1263.
24 B. Dahiya and P. K. Mehta, *Anal. Biochem.*, 2019, **587**, 11344.
25 X. Sun, R. Fei, L. Zhang, B. Huo, Y. Wang, Y. Peng, B. Ning, J. He, Z. Gao and Y. Hu, *Microchim. Acta*, 2020, **187**, 127.
26 M. Zhang, B. Huo, S. Yuan, B. Ning, J. Bai, Y. Peng, B. Liu and Z. Gao, *Anal. Chim. Acta*, 2018, **1043**, 98–106.
27 Y. Xu, B. Huo, C. Li, Y. Peng, S. Tian, L. Fan, J. Bai, B. Ning and Z. Gao, *Food Chem.*, 2019, **283**, 338–344.
28 A. Narmani, M. Kamali, B. Amini, H. Kooshki, A. Amini and L. Hassani, *Process Biochem.*, 2018, **65**, 46–54.
29 D. Manikandan, V. Jeyachandran and A. Manikandan, *Int. J. Pure Appl. Math.*, 2018, **119**, 265–278.
30 P. Rostron, T. Pennance, F. Bakar, D. Rollinson, S. Knopp, F. Allan, F. Kabole, S. M. Ali, S. M. Ame and B. L. Webster, *Parasites Vectors*, 2019, **12**, 514.
31 A. Garrido-Maestu, S. Azinheiro, P. Fuciños, J. Carvalho and M. Prado, *Food Microbiol.*, 2020, **92**, 103570.
32 J. S. McQuillan and M. W. Wilson, *Lett. Appl. Microbiol.*, 2021, **72**, 382–389.
33 J. Li, N. M. Pollak and J. Macdonald, *ACS Omega*, 2019, **4**, 11388–11396.
34 J. Ren, Y. Man, A. Li, G. Liang, X. Jin and L. Pan, *J. Food Saf.*, 2020, **40**, e12784.
35 H. Liu, J. Wang, H. Zeng, X. Liu, W. Jiang, Y. Wang, W. Ouyang and X. Tang, *Food Chem.*, 2021, **334**, 127608.
36 X. Ding, K. Yin, Z. Li, R. V. Lalla, E. Ballesteros, M. M. Sfeir and C. Liu, *Nat. Commun.*, 2020, **11**, 4711.
37 R. Aman, A. Mahas, T. Marsic, N. Hassan and M. M. Mahfouz, *Front. Microbiol.*, 2020, **11**, 610872.
38 Y. Sun, H. Liu, Y. Shen, X. Huang, F. Song, X. Ge, A. Wang, K. Zhang, Y. Li, C. Li, Y. Wan and J. Li, *ACS Omega*, 2020, **5**, 14814–14821.
39 X. Li, C. Zhao, Y. Liu, Y. Li, F. Lian, D. Wang, Y. Zhang, J. Wang, X. Song, J. Li, Y. Yang and K. Xu, *Analyst*, 2019, **144**, 2704–2715.
40 B. Wang, R. Wang, D. Wang, J. Wu, J. Li, J. Wang, H. Liu and Y. Wang, *Anal. Chem.*, 2019, **91**, 12156–12161.
41 M. Hu, C. Yuan, T. Tian, X. Wang, J. Sun, E. Xiong and X. Zhou, *J. Am. Chem. Soc.*, 2020, **142**, 7506–7513.
42 J. S. Chen, E. Ma, L. B. Harrington, M. Da Costa, X. Tian, J. M. Palefsky and J. A. Doudna, *Science*, 2018, **360**, 436–439.